ELSEVIER

Journal of Alloys and Compounds 235 (1996) 97–103

Journal of ALLOYS AND COMPOUNDS

Studies on the interactions of transition metal oxides and sodium sulfate in the temperature range 900–1200 K in oxygen

M. Mobin, A.U. Malik[1]

Department of Applied Chemistry, Z.H. College of Engineering and Technology, Aligarh Muslim University, Aligarh-202002, India

Received 12 May 1995; in final form 25 October 1995

Abstract

The interaction of different transition metal oxides such as TiO_2, ZrO_2, Nb_2O_5, MoO_3 and WO_3 with Na_2SO_4 in the temperature range 900–1200 K in flowing oxygen has been studied. The oxides chosen for the studies are initial scaling products during the oxidation of industrial alloys and are invariably involved in hot corrosion reactions in the presence of a molten salt. Thermogravimetric studies were carried out by measuring weight change as a function of time and molar fraction of Na_2SO_4 in the reaction mixture. The different constituents in the reaction products were identified by X-ray diffraction analysis and the morphologies of the reaction products were discussed on the basis of metallography, scanning electron microscopy and energy dispersive X-ray analysis. Quantitative estimation of soluble metal has also been carried out with the help of an atomic absorption spectrophotometer. Information regarding the formation of different species in the reaction product is also obtained from the study of relevant thermodynamic phase stability diagrams.

The high temperature reaction product usually contains a three-phase structure, namely sodium metal oxide, metal oxide and metal sulfide. The concentrations of the various constituents vary according to the composition of the interacting species, e.g. metal oxide and Na_2SO_4.

Keywords: Transition metal oxides; Interaction with sodium sulphate

1. Introduction

The excellent high temperature oxidation resistance of Fe-, Ni- or Co-based alloys is seriously affected when adherent protective scales are attacked by an electrolytic deposit. This type of attack, which causes degradation of an alloy at elevated temperatures, is called hot corrosion. A wide variety of electrolytic deposits, which include alkali and alkaline earth sulfates, chlorides, carbonates and vandates, are known to cause hot corrosion, but Na_2SO_4 has received greatest attention due to its involvement in actual engineering systems. Since the early 1970s considerable work has been reported on the influence of alloy additions on the hot corrosion behavior of high temperature alloys. For example, Goebel et al. [1] examined hot corrosion of Ni-based alloys containing Cr, Al, Mo, W and V additions, Stringer [2] discussed it at length in an excellent review and Rapp et al. published a later review [3]. Many references are available dealing with the phenomenology of Na_2SO_4-induced hot corrosion attack, but our knowledge regarding the chemical reactions taking place between molten Na_2SO_4 and the scales on the alloy consisting of slow growing oxides of $Cr_2O_3/Al_2O_3/SiO_2$ or the oxides of common alloying additions, which are usually present in the outer oxide layers, is rather limited. One of the factors that affects the oxidation resistance of the protective oxide scales is the solubility of the protective metal oxide in molten Na_2SO_4. However, only a limited amount of work has been carried out concerning the solubility of metal oxides in Na_2SO_4, which is closely related to the metal oxide–Na_2SO_4 interactions. Information regarding the interaction between a pertinent oxide and Na_2SO_4 and proper identification of reaction products should be useful in understanding the occurrence and importance of fluxing reactions, and thus in the interpretation of hot corrosion mechanism and in the development of new protective materials. The dissolution behavior of metal

[1] Corrosion Research Centre, SWCC, Al-Jubail, KSA.

SSDI 0925-8388(95)02125-6

oxide is important in explaining the electrochemical mechanism of hot corrosion in which soluble metal species are involved. The solubilities of several important metal oxides such as NiO, Co_3O_4, αAl_2O_3, Cr_2O_3, αFe_2O_3, SiO_2 and Y_2O_3 [4–9] were measured in molten Na_2SO_4 at 1200 K. Rapp [10] in his Whitney award lecture presented a compilation of measured solubilities in fused Na_2SO_4 at 1200 K for $P_{O_2} = 1$ atm. for the oxides of principal interest to high temperature alloys and coatings and emphasized the importance of local chemistry within a fused salt film. The results of a study of the high temperature interactions of some transition and non-transition metal oxides with NaCl, and some transition metal carbides separately with Na_2SO_4 and NaCl, have recently been published [11–13]. The presence of sodium metal oxide and metal sulfide/metal chloride in the reaction product has been confirmed in the above studies.

This paper presents the results of a study concerning the interaction of transition metal oxides and Na_2SO_4 in the temperature range 900–1200 K, where hot corrosion reactions are most active. The oxides chosen are those of metals present as alloy additions in industrial heat resistant alloys and they play a significant role in improving the high temperature mechanical and oxidation properties; these oxides undergo basic fluxing reactions.

2. Experimental details

Transition metal oxides TiO_2, ZrO_2, Nb_2O_5, Ta_2O_5, MoO_3 and WO_3 were all A.R. grade products. Analytical grade Na_2SO_4 was dried in an oven at 473 K for about 48 h. Dried and powdered Na_2SO_4 and the oxide (about 80 mesh size) were mixed separately in 1:2, 2:3, 1:1, 3:2 and 2:1 molar ratios and were compacted mechanically into a 1.4 cm tablet using a pressure of 10^7 kg m^{-2}.

The kinetics of high temperature reaction between Na_2SO_4 and metal oxides were studied by carrying out weight change vs. time measurements in the temperature range of 900–1200 K in a stream of pure and dried oxygen gas using a hot stage Sartorius electronic microbalance. A 24 h oxidation run was adequate to provide reaction product under steady state, which was indicated by a negligible change in weight for a considerable period of exposure time. To obtain a sufficient number of samples of the reaction products for a particular system, silica boats, each containing compacts of the same ratio, were placed in a horizontal furnace and oxidized under almost identical conditions. After completion of an oxidation run, the compacts were taken out, quenched in air and weighed. The oxidation samples were used for morphological studies (metallography, scanning electron microscopy (SEM) and energy dispersive X-ray analysis (EDAX)), X-ray diffraction (XRD) and quantitative estimation of soluble metal.

Metallographic studies were carried out on a computerized Leitz photometallurgical microscope (Metallux 2). The reaction products present in the form of compacts were mounted in paper moulds using Araldite as a cold setting resin. The mounted specimens were ground sequentially on different grit SiC papers, followed by polishing with 6 μm diamond paste using kerosine as the lapping liquid. Appropriate etchants [11] were used to identify the different phases in the microstructures.

The SEM and EDAX studies were performed using a Jeol electron microscope with an EDAX attachment, the XRD studies using an X-ray diffractometer, model APD1700 with Cu Kα or Mo Kα targets and appropriate filters.

The concentration of metal in the aqueous solution of reaction products for the system MoO_3–Na_2SO_4 (900 K) was determined with the help of varian atomic absorption spectrophotometer model AA975. The compact of the reaction products was weighed and dissolved in a fixed volume of demineralized water. The mixture was heated near to boiling, followed by filtration through a Whatman filter paper. The filtrate was diluted accordingly, and the concentration of metal was determined.

3. Results

3.1. Thermogravimetric studies

3.1.1. Reaction kinetics

Weight loss vs. time plots obtained during the reaction of 1:1 mixture of metal oxide and Na_2SO_4 in oxygen are shown in Fig. 1. With the exception of Nb_2O_5–Na_2SO_4, where there is a rapid weight loss up to 8 h, all the systems show a gradual weight loss up to 4–6 h with no further change in weight on exposure to oxygen.

3.1.2. Influence of salt

Fig. 2 shows plots of percentage total weight loss vs. molar fraction of Na_2SO_4 in the mixture of metal oxide and Na_2SO_4. The total weight loss represents the final reading recording after heating for 24 h of a mixture of metal oxide and Na_2SO_4 of known composition in the temperature range 900–1200 K in flowing oxygen. The weight loss incurred during a run of 24 h represents the total weight loss at steady state since no perceptible change in weight was observed after 24 h.

A study of the weight loss curves indicates three types of behavior during the interactions. The first showing no significant change in total weight loss values on varying Na_2SO_4 concentration in the re-

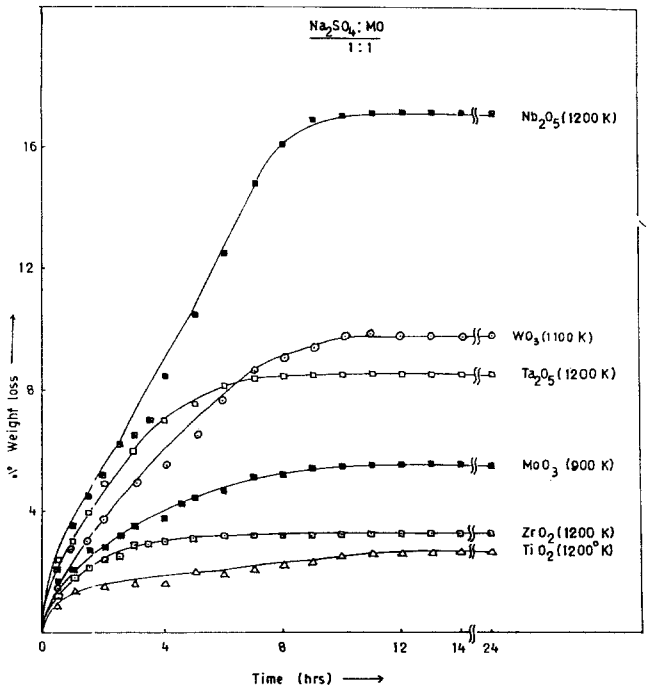

Fig. 1. Plots of percentage weight loss vs. time for 1:1 (molar ratio) Na_2SO_4–metal oxide systems.

action mixture and including TiO_2–Na_2SO_4 (1100 K), ZrO_2–Na_2SO_4 (1100 K), Ta_2O_5–Na_2SO_4 (1100 and 1200 K) and WO_3–Na_2SO_4 (1000 K). The second showing a minimum in the weight loss curves TiO_2–Na_2SO_4 (1200 K), Nb_2O_5–Na_2SO_4 (1100 K), MoO_3–Na_2SO_4 (900 K) and WO_3–Na_2SO_4 (1100 K). Lastly, the third showing a continuous increase in weight loss values with increasing amount of Na_2SO_4 and including ZrO_2–Na_2SO_4 (1200 K) and Nb_2O_5–Na_2SO_4 (1200 K).

3.1.3. Morphology of the reaction products

Figs. 3–8 show some representative photomicrographs of the mounted reaction products. In general, at lower concentration of Na_2SO_4 there is a relatively large concentration of species containing metal ions in the form of sulfates or sulfides in an oxide matrix, these appear in the form of dark or light phases in the photomicrographs. With increasing amount of Na_2SO_4 in the mixture, a light gray phase, which is a product of Na_2O and metal oxide, appears in the photomicrographs along with metal oxides. The EDAX results show an average distribution of elements in the form of energy diagrams (Figs. 9, 10).

Table 1 lists the different constituents as identified in the reaction products of 2:1 and 1:2 molar ratio of metal oxide and Na_2SO_4 by X-ray diffraction analysis.

3.1.4. Estimation of soluble metal

Taking the Na_2SO_4–MoO_3 system as a typical case, Table 2 provides metal solubility data at 900 K.

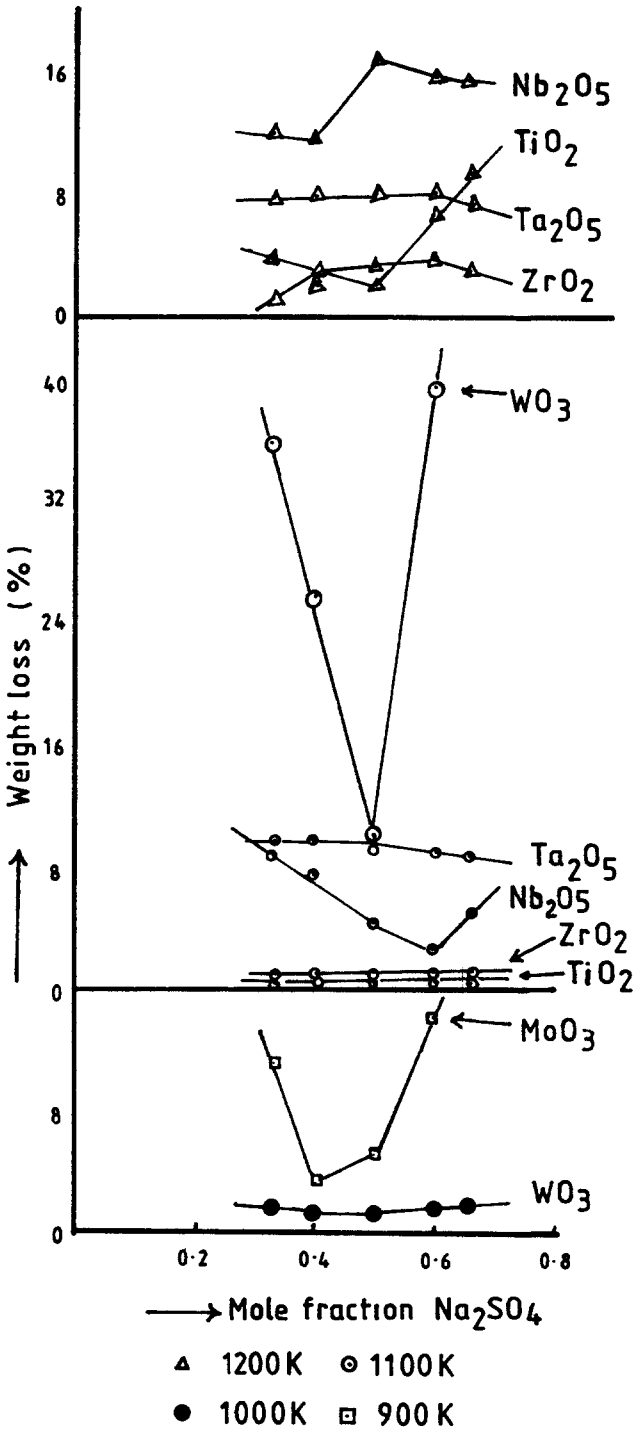

Fig. 2. Plots of percentage total weight loss vs. molar fraction of Na_2SO_4 for different Na_2SO_4–metal oxide systems.

4. Discussion

The high temperature interaction of Na_2SO_4 and transition metal oxides results in weight losses. The steady condition during kinetic measurements is indicated by a constant weight with increasing exposure time. The weight loss observed for all the systems is presumably due to the thermal decomposition of salt to Na_2O and subsequent expulsion of SO_2/SO_3 (g)

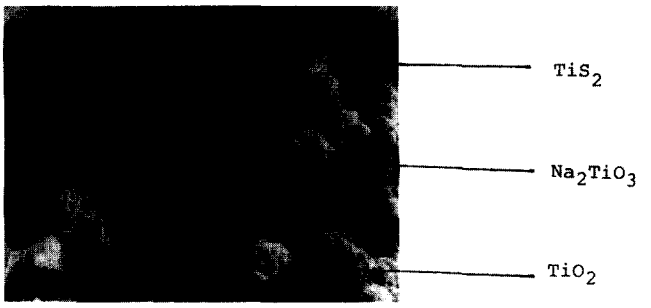

Fig. 3. SEM picture of 1:1 Na_2SO_4–TiO_2 reaction product oxidized at 1100 K.

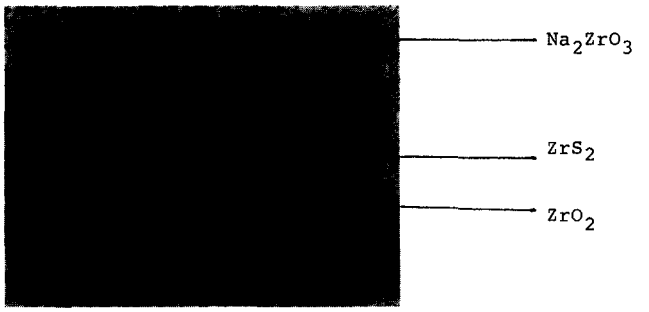

Fig. 4. SEM picture of 2:1 Na_2SO_4–ZrO_2 reaction product oxidized at 1100 K.

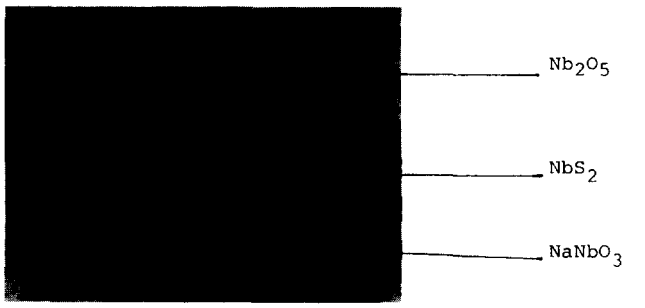

Fig. 5. SEM picture of 1:1 Na_2SO_4–Nb_2O_5 reaction product oxidized at 1200 K.

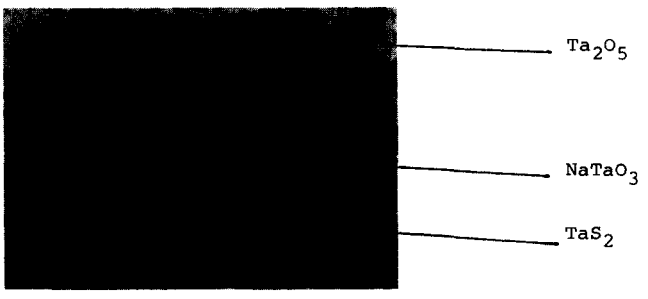

Fig. 6. SEM picture of 1:2 Na_2SO_4–Ta_2O_5 reaction product oxidized at 1200 K.

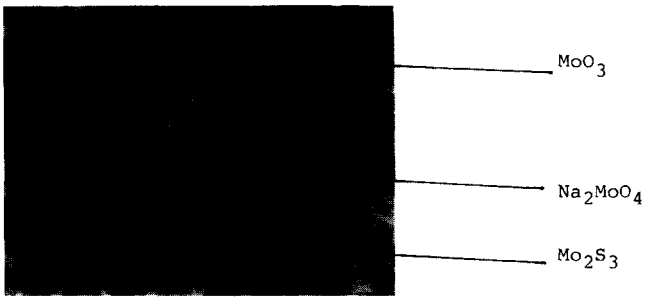

Fig. 7. SEM picture of 2:1 Na_2SO_4–MoO_3 reaction product oxidized at 900 K.

Fig. 8. Photomicrograph of 1:1 Na_2SO_4–WO_3 reaction product oxidized at 1000 K.

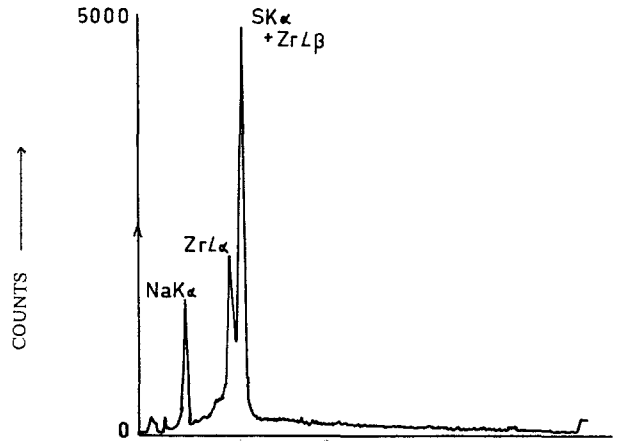

Fig. 9. X-ray energy profile diagram showing elemental distribution in the reaction product of 1:1 Na_2SO_4–ZrO_2 oxidized at 1100 K.

and some volatile compounds formed during the interactions. This is represented by the following general reactions:

$$Na_2SO_4(s) \rightleftharpoons Na_2O(s) + S(1) + 3/2\ O_2(g) \quad (I)$$

$$Na_2SO_4(s) \rightleftharpoons Na_2O(s) + SO_2(g) + 1/2\ O_2(g) \quad (IIa)$$

$$Na_2SO_4(s) \rightleftharpoons Na_2O(s) + SO_3(g) \quad (IIb)$$

If the thermodynamic conditions permit, then the Na_2O formed may dissolve metal oxide to give sodium metal oxide and sulfur and/or S-oxide gases may react with metal oxide giving metal sulfide and/or metal

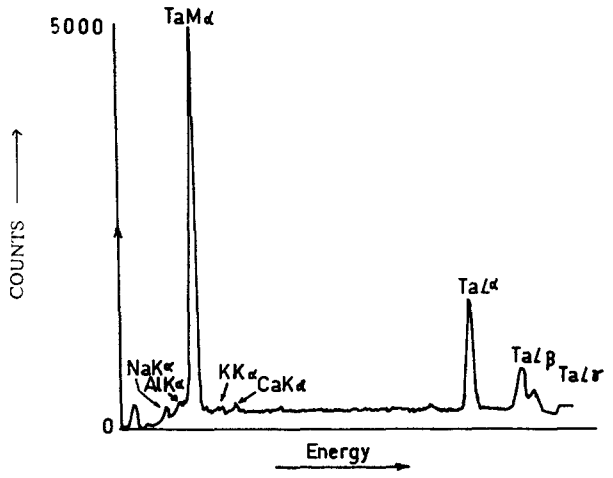

Fig. 10. X-ray energy profile diagram showing elemental distribution in the reaction product of 1:1 Na_2SO_4–Ta_2O_5 oxidized at 1100 K.

sulfate. This can be represented by the following general reactions:

$$Na_2O + MO \rightarrow Na_2O \cdot MO \quad \text{(III)}$$

$$MO + S \rightarrow MS + 1/2\ O_2 \quad \text{(IV)}$$

$$MO + SO_3 \rightarrow MSO_4 \quad \text{(V)}$$

The various species formed during the interaction can be written with the help of the above equations.

Studying the weight loss as a function of molar fraction of Na_2SO_4 in the mixture, three types of behavior were noted. In the first type virtually the same amount of weight loss was observed irrespective of the amount of Na_2SO_4 present in the mixture. This could be attributed to the absence of complete interaction between Na_2SO_4 and metal oxide at the experimental temperature. The initial weight loss in each case is due to expulsion of SO_2/SO_3(g) during the

Table 1
Different constituents identified in the reaction product by XRD analysis

System	Molar ratio	Temperature (K)	Constituents identified
TiO_2–Na_2SO_4	2:1	1100	Na_2SO_4, Na_2TiO_3, TiO_2
	1:2	1100	Na_2SO_4, Na_2TiO_3
	2:1	1200	Na_2SO_4, Na_2TiO_3, TiO_2
	1:2	1200	Na_2SO_4, Na_2TiO_3
ZrO_2–Na_2SO_4	2:1	1100	ZrO_2, ZrS, ZrS_2, Na_2SO_4, Na_2ZrO_3
	1:2	1100	ZrO_2, ZrS, ZrS_2, Na_2S, Na_2ZrO_3
	2:1	1200	ZrO_2, ZrS, Na_2ZrO_3
	1:2	1200	ZrO_2, Na_2S, ZrS, ZrS_2, Na_2ZrO_3
Nb_2O_5–Na_2SO_4	2:1	1100	Nb_2O_5, Na_2SO_4
	1:2	1100	Nb_2O_5, Na_2SO_4
	2:1	1200	Nb_2O_5, Na_2SO_4, $NaNbO_3$
	1:2	1200	$NaNbO_3$, Na_2SO_4
Ta_2O_5–Na_2SO_4	2:1	1100	TaS_2, Ta_2O_5, $NaTaO_3$
	1:2	1100	$NaTaO_3$, TaS_2, Na_2SO_4
	2:1	1200	TaS_2, Ta_2O_5, $NaTaO_3$
	1:2	1200	$NaTaO_3$, TaS_2, Na_2SO_4
MoO_3–Na_2SO_4	2:1	900	MoO_3, Na_2S, Na_2MoO_4, Mo_2S_3, Na_2SO_4
	1:2	900	Mo_2S_3, Mo_3S_2, MoO_3, Na_2MoO_4, Na_2SO_4
WO_3–Na_2SO_4	2:1	1000	WO_3, Na_2S, Na_2SO_4, Na_2WO_4
	1:2	1000	WO_3, Na_2S, WS_2, Na_2WO_4

Table 2
Metal solubility data for the Na_2SO_4–MoO_3 system at 900 K

Molar ratio Na_2SO_4:MoO_3	Weight of the reaction product (g)	Theoretical weight of the reaction mixture (g)		Concentration of soluble metal (ppm)
		Na_2SO_4	Metal oxide	
1:2	0.746	0.246	0.50	1731
1:1	0.490	0.243	0.247	5636
2:1	0.695	0.465	0.230	5974

overall reaction between Na_2SO_4 and metal oxide. In the second type, the total weight loss decreases with increasing amount of Na_2SO_4 in the mixture until a minimum is obtained, followed by an increase in weight loss values. Type three includes those systems which show a continuous increase in weight loss values with increasing amount of Na_2SO_4 in the mixture. The most plausible explanation for the above observations seems to be that a decrease in weight loss value with increasing amount of Na_2SO_4 is due to less formation of $SO_2/SO_3(g)$ or more binding of sulfur in the form of sulfide or sulfate. An increase in the weight loss with increasing amount of Na_2SO_4 is due to release of $SO_2/SO_3(g)$ and volatility of reaction products in certain cases.

The photomicrographs of the reaction products show the presence of multiphase structures. Each phase represents a constituent usually identified by XRD and predicted by proposed reactions. In general, an oxide phase or Na_2SO_4 appears as white, the reaction product $Na_2O \cdot MO$ as gray or light gray flocculant/granular and a sulfide as a dark phase.

From the available solubility data there is ample evidence of the formation of Na_2MoO_4 in the MoO_3–Na_2SO_4 system, as confirmed by XRD analysis.

Since both oxygen and sulfur participate in the reaction between metal oxides and Na_2SO_4, it is useful to employ Pourbaix type phase stability diagrams using log P_{O_2} vs. log a_{Na_2O} (P_{SO_3}) coordinates. With sufficient thermodynamic data, the behavior of metal oxide-fused salt systems may be described in terms of phase stability diagrams. In the construction of such diagrams, ideal behavior is assumed, and the activity

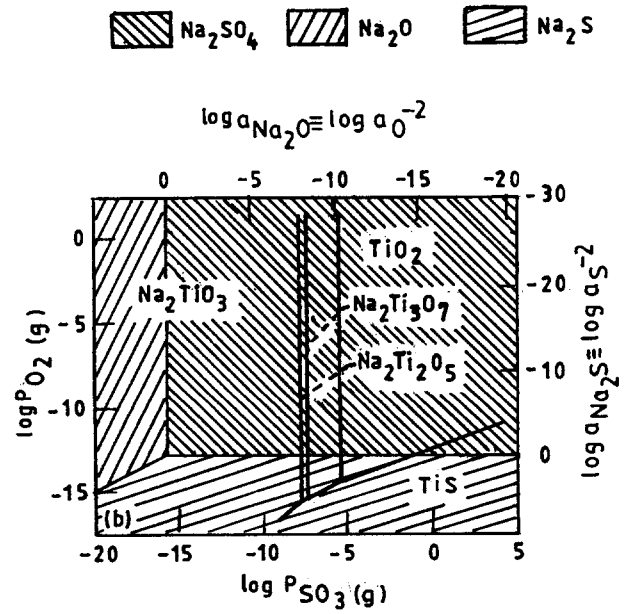

Fig. 11. Thermodynamic phase stability diagram [14] for the Na–Ti–S–O system at 1248 K. The dashed line is drawn where log a_{Na_2O} = log $P_{SO_3(g)}$.

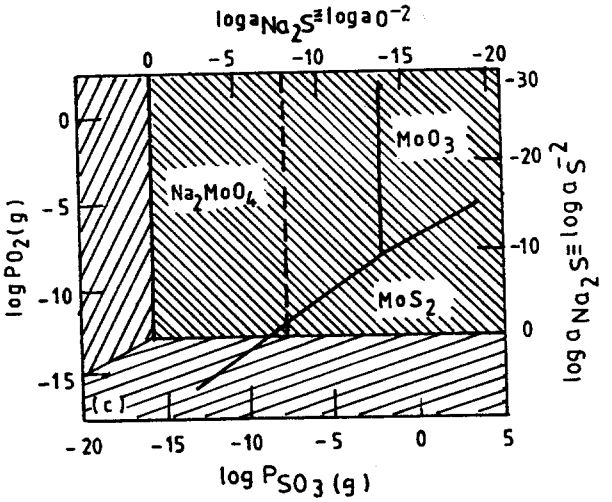

Fig. 12. Thermodynamic phase stability diagram [14] for the Na–Mo–S–O system at 1248 K. The dashed line is drawn where log a_{Na_2O} = log $P_{SO_3(g)}$.

of fused salt is considered to be unity. The activities of condensed phases are also considered to be unity in the regimes of thermodynamic stability. Figs. 11–13 [14] represent the phase stability diagrams for the system Na–Ti–S–O, Na–Mo–S–O and Na–W–S–O at 1248 K constructed by superimposing the Na–S–O diagram on the respective M–S–O diagrams. Referring to these diagrams, in pure oxygen atmosphere (log $P_{O_2} = 0$) Na_2TiO_3, Na_2MoO_4 and Na_2WO_4 are predominant species at higher Na_2SO_4 concentrations. In the present studies, evidence of the formation of

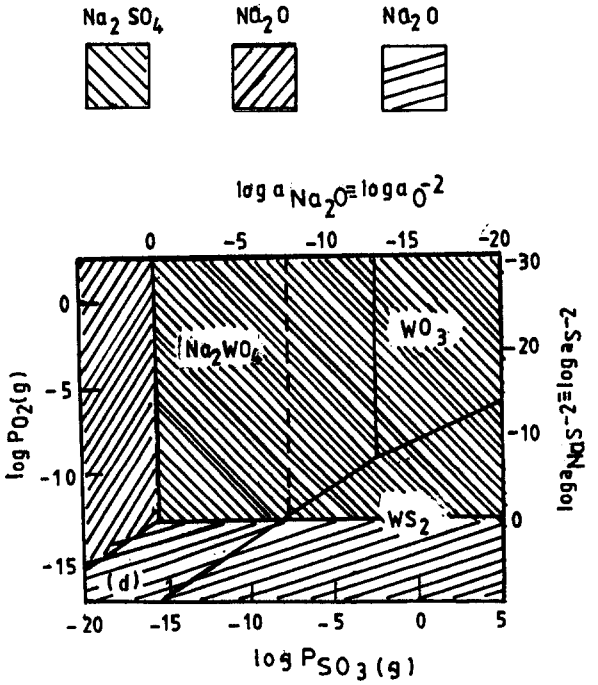

Fig. 13. Thermodynamic phase stability diagram [14] for the Na–W–S–O system at 1248 K. The dashed line is drawn where log a_{Na_2O} = log $P_{SO_3(g)}$.

these species has been obtained by XRD. No relevant Na–M–S–O thermodynamic phase stability diagrams are available for the system Na–Nb–S–O, Na–Ta–S–O and Na–Zr–S–O, but the evidence for the formation of solid constituents $NaNbO_3$, $NaTaO_3$ and Na_2ZrO_3 respectively, is obtained through XRD. The formation of $NaNbO_3$ and $NaTaO_3$ has been mentioned by Fryburg et al. [14] during the hot corrosion of Ni-based alloys.

5. Conclusions

(1) The interaction of Na_2SO_4 and transition metal oxides at high temperature results in weight losses indicating the expulsion of S-oxide gases and/or vaporization of some volatile compounds.

(2) Sodium metal oxide ($Na_2O \cdot MO$) and metal sulfides are usual products during the interactions.

(3) Determination of soluble metal in the aqueous solution of MoO_3–Na_2SO_4 reaction product indicates the presence of MoO_4^{2-} oxyanion.

(4) The constituents in the reaction product appear in the form of discrete and distinct phases in the optical and scanning micrographs.

References

[1] J.A. Goebel, F.S. Pettit and G.W. Goward, *Metall. Trans.*, *4* (1973) 261.
[2] J. Stringer, *Annu. Rev. Mater. Sci.*, *7* (1977) 477–509.
[3] R.A. Rapp, J.H. Devan, D.L. Douglass, P.C. Nordine, F.S. Pettit and D.P. Whittle, High temperature corrosion in energy systems, *Mater. Sci. Eng.*, *50* (1981) 1–17.
[4] D.K. Gupta and R.A. Rapp, *J. Electrochem. Soc.*, *127* (1980) 2194, 2656.
[5] P.D. Jose, D.K. Gupta and R.A Rapp, *J. Electrochem. Soc.*, *132* (1985) 735.
[6] Y.S. Zhang, *J. Electrochem. Soc.*, *133* (1986) 655.
[7] Y.S. Zhang and R.A. Rapp, *J. Electrochem. Soc.*, *132* (1985) 734, 2498.
[8] D.Z. Shi and R.A. Rapp, *J. Electrochem. Soc.*, *133* (1986) 849.
[9] M.L. Deanhardt and K.H. Stern, *Electrochim. Acta*, *129* (1982) 2228.
[10] R.A. Rapp, *Corros.-NACE*, *42* (1986) 568.
[11] M. Mobin, A.U. Malik and S. Ahmad, *J. Less-Common Met.*, *160* (1990) 1–14.
[12] M. Mobin and A.U. Malik, *J. Less-Common Met.*, *170* (1991) 243.
[13] M. Mobin and A.U. Malik, *J. Alloys Comp.*, *186* (1992) 1–14.
[14] G.C. Fryburg, F.J. Kohl, C.A. Stearns and W.L. Fiedler, *J. Electrochem. Soc.*, *131* (1984) 2985.